

Evolution of Tau-Neutrino Lepton Number in Protoneutron Stars due to Active-Sterile Neutrino Mixing

Anupam Ray ^{1,2,*} and Yong-Zhong Qian ^{2,†}

¹*Department of Physics, University of California Berkeley, Berkeley, California 94720, USA*

²*School of Physics and Astronomy, University of Minnesota, Minneapolis, MN 55455, USA*

(Dated: June 16, 2023)

We present an approximate treatment of the mixing between ν_τ ($\bar{\nu}_\tau$) and a sterile species ν_s ($\bar{\nu}_s$) with a vacuum mass-squared difference of $\sim 10^2\text{--}10^3$ keV² in protoneutron stars created in core-collapse supernovae. Including production of sterile neutrinos through both resonant flavor conversion and collisions, we track the evolution of the ν_τ lepton number due to both escape of sterile neutrinos and diffusion. Our approach provides a reasonable treatment of the pertinent processes discussed in previous studies and serves a pedagogical purpose to elucidate the relevant physics. We also discuss refinements needed to study more accurately how flavor mixing with sterile neutrinos affects protoneutron star evolution.

I. INTRODUCTION

Sterile neutrinos associated with a vacuum mass eigenstate of $\mathcal{O}(10)$ keV in mass have been studied extensively as a viable dark matter candidate [1–5]. Detection of an unidentified X-ray line near 3.55 keV by stacked observations of galaxy clusters and its possible explanation by the decay of sterile neutrinos [6, 7] have provided further stimulation for such studies. Among the exploration of the effects of sterile neutrinos in cosmology and astrophysics, a number of studies have investigated their flavor mixing with active neutrinos in core-collapse supernovae [8–19]. In this paper, we revisit this topic to gain more insights into the underlying processes. Specifically, we focus on the mixing between ν_τ ($\bar{\nu}_\tau$) and a sterile species ν_s ($\bar{\nu}_s$) with a vacuum mass-squared difference of $\delta m^2 \sim 10^2\text{--}10^3$ keV² in protoneutron stars created in core-collapse supernovae, and estimate the evolution of the ν_τ lepton number as a result of such mixing. Our purpose is mainly pedagogical. While the key effects of $\nu_\tau\text{--}\nu_s$ and $\bar{\nu}_\tau\text{--}\bar{\nu}_s$ mixing in protoneutron stars have been discussed by a number of previous studies (e.g., [12, 13, 16, 17, 19]), we wish to elucidate the underlying physics by examining various aspects of the problem, including assumptions and approximations made to facilitate a reasonable treatment.

The following previous studies are especially pertinent to our discussion. In Ref. [12], the formalism for treating production of sterile neutrinos through collisions of active neutrinos in the supernova core was developed. Ref. [13] pointed out that escape of ν_s ($\bar{\nu}_s$) mixed with ν_τ ($\bar{\nu}_\tau$) leads to evolution of the ν_τ lepton number, which tends to turn off the effects of such flavor mixing. Ref. [16] highlighted that $\bar{\nu}_\tau\text{--}\bar{\nu}_s$ conversion is greatly enhanced by the Mikheyev–Smirnov–Wolfenstein (MSW) effect [20, 21] when the neutrino mean free path exceeds the width of the resonance region. A careful numerical study of $\nu_\tau\text{--}\nu_s$

and $\bar{\nu}_\tau\text{--}\bar{\nu}_s$ mixing was carried out in Ref. [17] with emphasis on the feedback of such mixing. Finally, the effects of diffusion of the ν_τ lepton number created by such mixing were discussed in Ref. [19]. However, a concise and analytical treatment of all the relevant processes appears lacking, and we aim to present such an approach here.

The rest of the paper is organized as follows. In Section II we set up the problem of $\nu_\tau\text{--}\nu_s$ and $\bar{\nu}_\tau\text{--}\bar{\nu}_s$ mixing with $\delta m^2 \sim 10^2\text{--}10^3$ keV² in protoneutron stars. We discuss the production of sterile neutrinos through both the MSW effect and collisions, as well as the diffusion of the ν_τ lepton number created by such mixing. In Section III we present example calculations to illustrate the overall evolution of the ν_τ lepton number in protoneutron stars due to both escape of sterile neutrinos and diffusion. In Section IV we elaborate on the feedback of $\nu_\tau\text{--}\nu_s$ and $\bar{\nu}_\tau\text{--}\bar{\nu}_s$ mixing by focusing on the evolution of the ν_τ lepton number in a specific radial zone. In Section V we give conclusions and discuss refinements needed to study more accurately how flavor mixing with sterile neutrinos affects protoneutron star evolution.

II. ACTIVE-STERILE NEUTRINO MIXING IN PROTONEUTRON STARS

We consider the mixing of ν_τ ($\bar{\nu}_\tau$) and ν_s ($\bar{\nu}_s$) with $\delta m^2 \sim 10^2\text{--}10^3$ keV² and vacuum mixing angle $\theta \ll 1$. In protoneutron stars, forward scattering on electrons, protons, neutrons, and neutrinos results in a potential

$$V_\nu = \sqrt{2}G_F n_b \left[-\frac{1 - Y_e}{2} + Y_{\nu_e} + Y_{\nu_\mu} + 2Y_{\nu_\tau} \right] \quad (1)$$

for $\nu_\tau\text{--}\nu_s$ mixing, where G_F is the Fermi constant, n_b is the baryon number density, Y_e is the electron fraction (net number of electrons per baryon), $Y_{\nu_\alpha} = (n_{\nu_\alpha} - n_{\bar{\nu}_\alpha})/n_b$ with $\alpha = e, \mu,$ and τ is the ν_α -lepton number fraction, and n_{ν_α} ($n_{\bar{\nu}_\alpha}$) is the number density of ν_α ($\bar{\nu}_\alpha$). The corresponding potential for $\bar{\nu}_\tau\text{--}\bar{\nu}_s$ mixing is $V_{\bar{\nu}} = -V_\nu$. The above potentials modify the $\nu_\tau\text{--}\nu_s$ and $\bar{\nu}_\tau\text{--}\bar{\nu}_s$ mixing in protoneutron stars, which is character-

* anupam.ray@berkeley.edu

† qianx007@umn.edu

ized by the effective mixing angles θ_ν and $\theta_{\bar{\nu}}$, respectively. For a neutrino with energy E ,

$$\sin^2 2\theta_\nu = \frac{\Delta^2 \sin^2 2\theta}{(\Delta \cos 2\theta - V_\nu)^2 + \Delta^2 \sin^2 2\theta}, \quad (2)$$

$$\sin^2 2\theta_{\bar{\nu}} = \frac{\Delta^2 \sin^2 2\theta}{(\Delta \cos 2\theta - V_{\bar{\nu}})^2 + \Delta^2 \sin^2 2\theta}, \quad (3)$$

where $\Delta = \delta m^2/(2E)$.

For conditions in protoneutron stars, $V_\nu < 0$ and $V_{\bar{\nu}} > 0$, so ν_τ - ν_s mixing is suppressed but there is a resonance for $\bar{\nu}_\tau$ - $\bar{\nu}_s$ mixing when $\Delta \cos 2\theta = V_{\bar{\nu}}$. For $\theta \ll 1$, the resonance energy E_R corresponding to a specific value of $V_{\bar{\nu}}$ is

$$E_R = \frac{\delta m^2}{2V_{\bar{\nu}}} = \frac{13.1 \text{ MeV}(\delta m^2/10^2 \text{ keV}^2)}{(1 - Y_e - 2Y_{\nu_e} - 2Y_{\nu_\mu} - 4Y_{\nu_\tau})\rho_{14}}, \quad (4)$$

where ρ_{14} is the mass density in units of $10^{14} \text{ g cm}^{-3}$. By definition, the resonance region for a $\bar{\nu}_\tau$ with energy E_R corresponds to $\sin^2 2\theta_{\bar{\nu}} \geq 1/2$. For a radially-propagating $\bar{\nu}_\tau$, this region has a radial width

$$\delta r = 2H_R \tan 2\theta, \quad (5)$$

where $H_R = |\partial \ln V_{\bar{\nu}}/\partial r|_{E_R}^{-1}$ and the derivative is taken at the resonance radius for E_R . For $\theta \ll 1$, we can make the approximation that $\theta_{\bar{\nu}}$ changes from $\pi/2$ to 0 (or vice versa) once the resonance region is traversed and use the Landau-Zener formula (e.g., [22, 23]) to estimate the survival probability for a radially-propagating $\bar{\nu}_\tau$ as

$$P_{\text{LZ}} = \exp\left(-\frac{\pi^2 \delta r}{2L_{\text{res}}}\right) = e^{-\gamma_R}, \quad (6)$$

where

$$L_{\text{res}} = \frac{4\pi E_R}{\delta m^2 \sin 2\theta} \quad (7)$$

is the oscillation length at resonance and

$$\gamma_R = 39.8 \left(\frac{\sin^2 2\theta}{10^{-10}}\right) \left(\frac{\delta m^2}{10^2 \text{ keV}^2}\right) \left(\frac{\text{MeV}}{E_R}\right) \left(\frac{H_R}{\text{km}}\right) \quad (8)$$

is the adiabaticity parameter. For $\gamma_R \gg 1$, flavor evolution is highly adiabatic with $P_{\text{LZ}} \sim 0$ and $\bar{\nu}_\tau$ is efficiently converted into $\bar{\nu}_s$.

Description of ν_s and $\bar{\nu}_s$ production requires knowledge about ν_τ and $\bar{\nu}_\tau$ in protoneutron stars. We focus on the region where all active neutrinos are diffusing and assume that they are always in local thermodynamic equilibrium with the matter background (i.e., neutrons, protons, electrons, positrons, and photons). Consequently, the ν_α and $\bar{\nu}_\alpha$ energy distributions (number densities per unit energy interval per unit solid angle) are

$$\frac{d^2 n_{\nu_\alpha}}{dE d\Omega} = \frac{1}{(2\pi)^3} \frac{E^2}{e^{(E - \mu_{\nu_\alpha})/T} + 1}, \quad (9)$$

$$\frac{d^2 n_{\bar{\nu}_\alpha}}{dE d\Omega} = \frac{1}{(2\pi)^3} \frac{E^2}{e^{(E + \mu_{\nu_\alpha})/T} + 1}, \quad (10)$$

where $d\Omega$ is the differential solid angle in the direction of the momentum, μ_{ν_α} is the ν_α chemical potential, and T is the matter temperature. The ν_α -lepton number fraction is

$$Y_{\nu_\alpha} = \frac{T^3 \eta_{\nu_\alpha}}{6n_b} \left(1 + \frac{\eta_{\nu_\alpha}^2}{\pi^2}\right), \quad (11)$$

where $\eta_{\nu_\alpha} = \mu_{\nu_\alpha}/T$. Protoneutron stars have $Y_{\nu_\mu} \ll Y_{\nu_e} \ll 1 - Y_e$ and we assume $Y_{\nu_\mu} = 0$ hereafter. Because we only consider ν_τ - ν_s and $\bar{\nu}_\tau$ - $\bar{\nu}_s$ mixing, neither Y_{ν_e} nor Y_{ν_μ} is affected by such mixing, but the feedback on Y_{ν_τ} is critical to our discussion.

For numerical examples, we use the protoneutron star conditions from a $20 M_\odot$ supernova model (with the SFHo nuclear equation of state) at 1 s post core bounce [24–27]. The corresponding radial profiles of ρ , T , Y_e , and Y_{ν_e} are shown in Fig. 1.

A. Sterile neutrino production through MSW effect

For a homogeneous medium with uniform density and temperature, sterile neutrinos are produced through collisions of active neutrinos only and the problem was treated in Ref. [13]. For realistic protoneutron stars, both density and temperature vary with radius (see Fig. 1). Ref. [16] highlighted that $\bar{\nu}_\tau$ can be resonantly converted into $\bar{\nu}_s$ through the MSW effect when the $\bar{\nu}_\tau$ mean free path is longer than the size of the resonance region δr . The mean free path is determined predominantly by neutral-current scattering on neutrons and protons for both ν_τ and $\bar{\nu}_\tau$. It can be estimated as

$$\lambda(E) = \frac{1}{n_b \sigma(E)} \approx \frac{9.85 \text{ km}}{\rho_{14}} \left(\frac{\text{MeV}}{E}\right)^2, \quad (12)$$

where $\sigma(E) \approx G_F^2 E^2/\pi$ is the cross section (e.g., [13]).

Denoting $\lambda_R = \lambda(E_R)$, we consider a volume element of linear size $l \sim \lambda_R > \delta r$ that surrounds the point of resonance for energy E_R . Inside this volume element, $\bar{\nu}_\tau$ with energy close to E_R and propagating radially outward can cross their resonance regions without encountering collisions and be converted into $\bar{\nu}_s$ with probability $1 - P_{\text{LZ}}$. Specifically, the energy interval of such $\bar{\nu}_\tau$ is

$$\delta E = \left|\frac{\partial E_R}{\partial r}\right| l = \frac{l}{H_R} E_R. \quad (13)$$

However, the angular distribution of $\bar{\nu}_\tau$ is isotropic [see Eq. (10)]. A $\bar{\nu}_\tau$ propagating with a polar angle $\vartheta \sim \pi/2$ relative to the radially outward direction experiences less change of $V_{\bar{\nu}}$ inside the volume element than a radially-propagating $\bar{\nu}_\tau$ and therefore, may fail to traverse its full resonance region before encountering collisions. In this

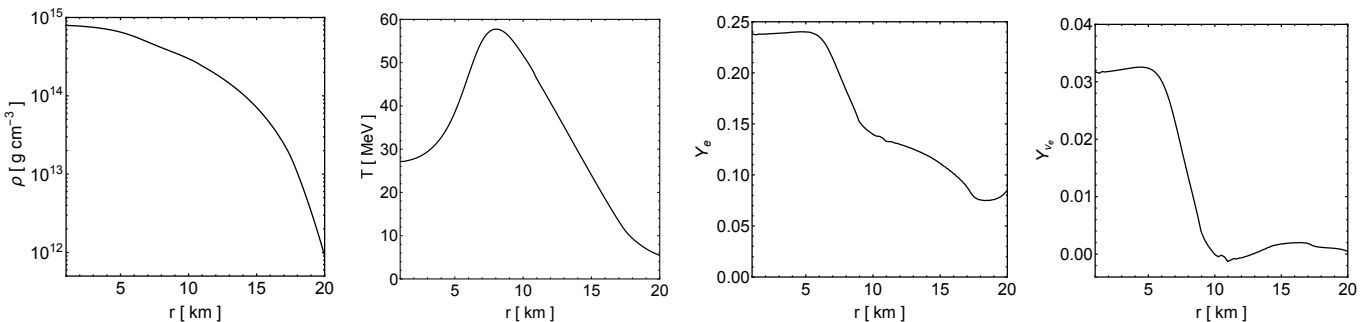


FIG. 1. Proton-neutron star conditions from a $20 M_{\odot}$ supernova model (with the SFHo nuclear equation of state) at 1 s post core bounce [24]. The radial profiles of ρ , T , Y_e , and Y_{ν_s} are shown.

case, the MSW effect would be reduced significantly because flavor evolution now depends on the specific values of $V_{\bar{\nu}}$ between successive collisions (i.e., we can no longer assume that $\theta_{\bar{\nu}}$ changes from $\pi/2$ to 0 or vice versa in crossing the resonance). In addition, a $\bar{\nu}_{\tau}$ propagating radially inward goes through a second resonance region on the opposite side of the proton-neutron star center.

While a full treatment should account for all the directional dependence of $\bar{\nu}_s$ production through the MSW effect, we provide an approximate treatment by considering the effective flux $\Phi_{\bar{\nu}_s}^{\text{MSW}}$ of $\bar{\nu}_s$ (number per unit area per unit time) escaping radially (both outward and inward) from the volume element. Because the contribution to this flux is weighed by $\cos\vartheta$, we assume that $\bar{\nu}_{\tau}$ with $0 \leq \vartheta < \pi/2$ ($\pi/2 < \vartheta \leq \pi$) experience the same MSW effect as a $\bar{\nu}_{\tau}$ propagating radially outward (inward). Taking into account that a $\bar{\nu}_{\tau}$ propagating radially inward goes through two resonance regions, we obtain

$$\begin{aligned} \Phi_{\bar{\nu}_s}^{\text{MSW}} &= \Theta(\lambda_R - \delta r)(1 - P_{\text{LZ}}) \left. \frac{d^2 n_{\bar{\nu}_{\tau}}}{dE d\Omega} \right|_{E_R} \delta E \\ &\times \left[\int_{\text{out}} d\Omega \cos\vartheta + P_{\text{LZ}} \int_{\text{in}} d\Omega |\cos\vartheta| \right] \quad (14) \end{aligned}$$

$$= \Theta(\lambda_R - \delta r) \pi (1 - P_{\text{LZ}}^2) \left. \frac{d^2 n_{\bar{\nu}_{\tau}}}{dE d\Omega} \right|_{E_R} \delta E, \quad (15)$$

where $\Theta(x)$ is the Heaviside step function. We then estimate that due to the MSW effect, the rate of change of $Y_{\nu_{\tau}}$ in the volume element is

$$\dot{Y}_{\nu_{\tau}}^{\text{MSW}} = \frac{\Phi_{\bar{\nu}_s}^{\text{MSW}}}{n_b l}, \quad (16)$$

$$= \Theta(\lambda_R - \delta r) \frac{\pi E_R (1 - P_{\text{LZ}}^2)}{n_b H_R} \left. \frac{d^2 n_{\bar{\nu}_{\tau}}}{dE d\Omega} \right|_{E_R}, \quad (17)$$

$$\begin{aligned} &= \frac{222 \text{ s}^{-1}}{\rho_{14}} \left(\frac{E_R}{30 \text{ MeV}} \right)^3 \left(\frac{\text{km}}{H_R} \right) \\ &\times \frac{\Theta(\lambda_R - \delta r)(1 - P_{\text{LZ}}^2)}{e^{(E_R/T) + \eta_{\nu_{\tau}}} + 1}. \quad (18) \end{aligned}$$

The above results are derived here for the first time, although they are qualitatively similar to those assumed

in Refs. [16, 17, 19]. Quantitatively, the rate of change of $Y_{\nu_{\tau}}$ due to the MSW effect used in the previous studies is approximately

$$\dot{Y}_{\nu_{\tau}}^{\text{MSW}'} = \Theta(\lambda_R - \delta r) \frac{4\pi E_R (1 - P_{\text{LZ}})}{n_b H_R} \left. \frac{d^2 n_{\bar{\nu}_{\tau}}}{dE d\Omega} \right|_{E_R}, \quad (19)$$

which assumes that $\bar{\nu}_{\tau}$ experience the same MSW effect regardless of their direction of propagation and therefore, is clearly an overestimate. While $\dot{Y}_{\nu_{\tau}}^{\text{MSW}}$ might be a more realistic estimate, we will present results using both $\dot{Y}_{\nu_{\tau}}^{\text{MSW}}$ and $\dot{Y}_{\nu_{\tau}}^{\text{MSW}'}$ for comparison.

B. Sterile neutrino production through collisions

In the same volume element considered in Section II A, non-resonant ν_{τ} and $\bar{\nu}_{\tau}$ can be converted into ν_s and $\bar{\nu}_s$, respectively, through flavor mixing and collisions (e.g., [12]). We take the resulting rate of change of $Y_{\nu_{\tau}}$ to be

$$\begin{aligned} \dot{Y}_{\nu_{\tau}}^{\text{coll}} &= \frac{\pi}{n_b} \left[\int_{E_{\bar{\nu}_{\tau}}} dE \frac{\sin^2 2\theta_{\bar{\nu}}}{\lambda(E)} \frac{d^2 n_{\bar{\nu}_{\tau}}}{dE d\Omega} \right. \\ &\left. - \int_0^{\infty} dE \frac{\sin^2 2\theta_{\nu}}{\lambda(E)} \frac{d^2 n_{\nu_{\tau}}}{dE d\Omega} \right], \quad (20) \end{aligned}$$

$$\begin{aligned} &= G_F^2 \left(\int_{E_{\bar{\nu}_{\tau}}} dE E^2 \sin^2 2\theta_{\bar{\nu}} \frac{d^2 n_{\bar{\nu}_{\tau}}}{dE d\Omega} \right. \\ &\left. - \int_0^{\infty} dE E^2 \sin^2 2\theta_{\nu} \frac{d^2 n_{\nu_{\tau}}}{dE d\Omega} \right), \quad (21) \end{aligned}$$

where the integration over $E_{\bar{\nu}_{\tau}}$ excludes the range $[E_R - \delta E/2, E_R + \delta E/2]$ with $\delta E = (\lambda_R/H_R)E_R$ for resonant $\bar{\nu}_{\tau}$ (see Fig. 2) when λ_R exceeds δr and goes from 0 to ∞ otherwise. The above rate is similar to that used in Ref. [13]. It corresponds to effective rates of $\sin^2 2\theta_{\nu}/[4\lambda(E)]$ and $\sin^2 2\theta_{\bar{\nu}}/[4\lambda(E)]$ for ν_s and $\bar{\nu}_s$ production by collisions of ν_{τ} and $\bar{\nu}_{\tau}$, respectively. Note that the effective $\bar{\nu}_s$ production rate also applies to resonant $\bar{\nu}_{\tau}$ when λ_R falls below δr .

Integrating over the full range of $E_{\bar{\nu}_{\tau}}$ and using $\sin^2 2\theta_{\bar{\nu}} \approx \pi E_R \delta(E - E_R) \tan 2\theta$, we estimate the con-

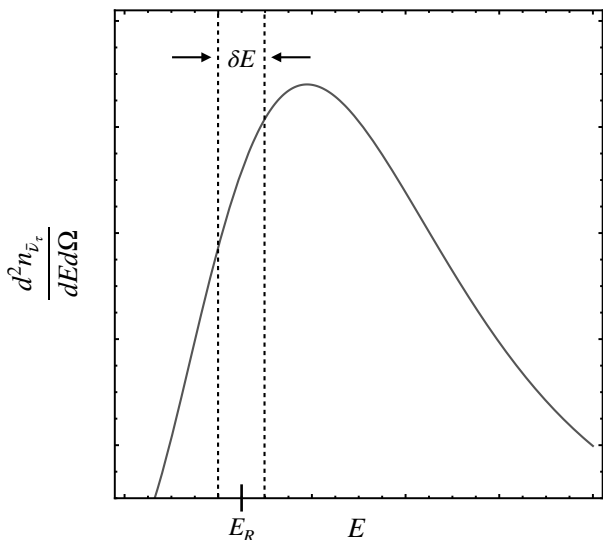


FIG. 2. Sketch of the $\bar{\nu}_\tau$ energy distribution at a specific radius. This distribution is determined by the T and μ_{ν_τ} at this radius. For a given set of mixing parameters, the potential $V_{\bar{\nu}}$ at this radius defines a resonance energy E_R . Inside a volume element of linear size λ_R centered at this radius, $\bar{\nu}_\tau$ with energy $[E_R - \delta E/2, E_R + \delta E/2]$ go through the MSW resonances. Here λ_R is the mean free path for $\bar{\nu}_\tau$ with energy E_R and $\delta E = (\lambda_R/H_R)E_R$ with $H_R = |\partial \ln V_{\bar{\nu}}/\partial r|_{E_R}^{-1}$.

tribution to $\dot{Y}_{\nu_\tau}^{\text{coll}}$ from $\bar{\nu}_\tau$ - $\bar{\nu}_s$ mixing to be

$$\dot{Y}_{\nu_\tau}^{\text{coll}, \bar{\nu}} \lesssim \frac{0.6 \text{ s}^{-1}}{e^{(E_R/T) + \eta_{\nu_\tau}} + 1} \left(\frac{E_R}{30 \text{ MeV}} \right)^5 \left(\frac{\sin 2\theta}{10^{-5}} \right). \quad (22)$$

Because $\sin^2 2\theta_\nu < \sin^2 2\theta$, the contribution to $\dot{Y}_{\nu_\tau}^{\text{coll}}$ from ν_τ - ν_s mixing is

$$\dot{Y}_{\nu_\tau}^{\text{coll}, \nu} < -2 \times 10^{-6} \text{ s}^{-1} \left(\frac{T}{30 \text{ MeV}} \right)^5 \left(\frac{\sin^2 2\theta}{10^{-10}} \right) F_4(\eta_{\nu_\tau}), \quad (23)$$

where $F_4(\eta_{\nu_\tau})$ is the Fermi-Dirac integral of rank 4 and argument η_{ν_τ} . In general,

$$F_k(\eta) = \int_0^\infty dx \frac{x^k}{e^{x-\eta} + 1}. \quad (24)$$

Comparing Eqs. (22) and (23) with (18), we expect that the rate of change of Y_{ν_τ} is dominated by $\dot{Y}_{\nu_\tau}^{\text{MSW}}$ when λ_R exceeds δr and that this rate decreases dramatically to $\dot{Y}_{\nu_\tau}^{\text{coll}}$ when λ_R falls below δr .

C. Diffusion of tau-neutrino lepton number

As we focus on the region where all active neutrinos are diffusing, the outer radius R_ν of this region is an important quantity. For a ν_τ or $\bar{\nu}_\tau$ of energy E , the transition from diffusion to free-streaming occurs at radius r for

which $\int_r^{R_*} dr/\lambda(E) \sim 1$ with R_* being the radius of the protoneutron star. Considering the energy distributions of ν_τ and $\bar{\nu}_\tau$, we estimate R_ν to be given by

$$\int_{R_\nu}^{R_*} \frac{dr}{\langle \lambda(E) \rangle_{\bar{\nu}_\tau}} = \frac{G_F^2}{\pi} \int_{R_\nu}^{R_*} dr n_b T^2 \frac{F_2(-\eta_{\nu_\tau})}{F_0(-\eta_{\nu_\tau})} = 1, \quad (25)$$

where $\langle \lambda(E) \rangle_{\bar{\nu}_\tau}$ is the mean free path averaged over the $\bar{\nu}_\tau$ energy distribution. The use of $\langle \lambda(E) \rangle_{\bar{\nu}_\tau}$ gives a more stringent estimate of R_ν , which typically corresponds to a density $\rho \sim 10^{13} \text{ g cm}^{-3}$.

The net ν_τ -lepton number flux crossing a surface at radius r in the radially outward direction is

$$\begin{aligned} \Phi_{\nu_\tau}(r) &= \int_0^\infty dE \frac{\lambda(E)}{3} \frac{\partial}{\partial r} \left(\frac{dn_{\bar{\nu}_\tau}}{dE} - \frac{dn_{\nu_\tau}}{dE} \right), \quad (26) \\ &= -\frac{1}{6\pi G_F^2 n_b} \frac{\partial \mu_{\nu_\tau}}{\partial r}. \quad (27) \end{aligned}$$

Due to the above diffusive flux, the rate of change of Y_{ν_τ} in the volume element considered in Section II A is

$$\dot{Y}_{\nu_\tau}^{\text{diff}} = \frac{1}{6\pi G_F^2 n_b r^2} \frac{\partial}{\partial r} \left(r^2 \frac{\partial \mu_{\nu_\tau}}{\partial r} \right). \quad (28)$$

This result is the same as that used in Ref. [19] when the typo in its Eq. (10) is corrected. As a crude estimate, the above rate is of the order $\sim 0.1 \text{ s}^{-1} \rho_{14}^{-2} (\partial^2 \mu_{\nu_\tau, \text{MeV}} / \partial r_{\text{km}}^2)$, where $\mu_{\nu_\tau, \text{MeV}}$ is μ_{ν_τ} in units of MeV and r_{km} is r in units of km. We expect that this rate is also small compared to $\dot{Y}_{\nu_\tau}^{\text{MSW}}$ when λ_R exceeds δr .

III. EXAMPLE CALCULATIONS

As discussed in Section II, treatment of ν_τ - ν_s and $\bar{\nu}_\tau$ - $\bar{\nu}_s$ mixing includes production of ν_s and $\bar{\nu}_s$ through the MSW effect and collisions, as well as diffusion of the resulting Y_{ν_τ} . In turn, the evolution of Y_{ν_τ} due to these processes changes the potentials V_ν and $V_{\bar{\nu}}$ for such mixing. Therefore, it is crucial to take this feedback into account in exploring the effects of such mixing. For illustration, we calculate the evolution of Y_{ν_τ} for $(m_s/\text{keV}, \sin^2 2\theta) = (7.1, 7 \times 10^{-11})$, $(10, 10^{-12})$, and $(30, 10^{-12})$, respectively, where $m_s \approx \sqrt{\delta m^2}$ is the mass of the vacuum mass eigenstate almost coincident with the sterile neutrino. The first set of parameters is suggested by interpreting the X-ray line emission near 3.55 keV from galaxy clusters as due to sterile neutrino decay [6, 7], while the second set is chosen for sterile neutrinos to make up all the dark matter [28, 29]. For $m_s = 30 \text{ keV}$, sterile neutrinos can make up all the dark matter for $\sin^2 2\theta \lesssim 10^{-14}$. Because the decay rate is proportional to $\sin^2 2\theta$, limits imposed by decay X-ray emission imply that sterile neutrinos can account for only $\lesssim 1\%$ of the dark matter for the third set of parameters [28, 29].

For the protoneutron star conditions, we take a snapshot of a $20 M_\odot$ supernova model (with the SFHo nuclear equation of state) at 1 s post core bounce [24–27]. We

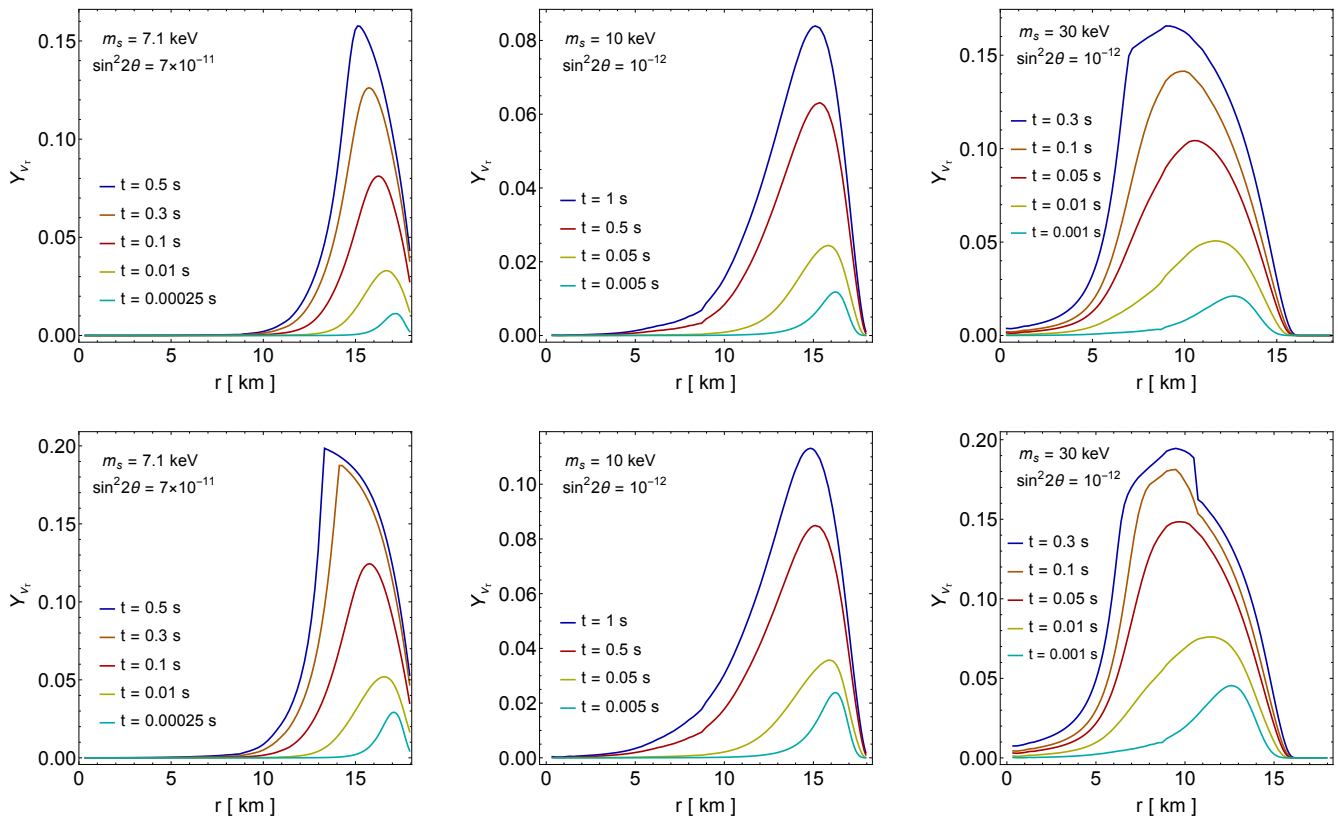


FIG. 3. Radial profile of Y_{ν_τ} at different times calculated for the indicated mixing parameters and for the protoneutron star conditions shown in Fig. 1. The top and bottom panels differ in the adopted rate of change of Y_{ν_τ} due to the MSW effect, with $\dot{Y}_{\nu_\tau}^{\text{MSW}}$ and $\dot{Y}_{\nu_\tau}^{\text{MSW}'}$ used for the former and latter, respectively.

assume that the radial profiles of ρ , T , Y_e , and Y_{ν_e} (see Fig. 1) remain static during our calculation. The evolution of $Y_{\nu_\tau}(r, t)$ for a specific radial zone is determined by

$$\frac{\partial Y_{\nu_\tau}}{\partial t} = \dot{Y}_{\nu_\tau}^{\text{MSW}} + \dot{Y}_{\nu_\tau}^{\text{coll}} + \dot{Y}_{\nu_\tau}^{\text{diff}}. \quad (29)$$

Using appropriate time steps, we obtain the radial profile of Y_{ν_τ} at different times from the above equation. Because this equation is valid when active neutrinos, especially ν_τ and $\bar{\nu}_\tau$, are in the diffusion regime, the radial profile of interest is up to $r = R_\nu$.

Using the three sets of mixing parameters given above, we show in Fig. 3 the radial profile of Y_{ν_τ} at different times ($t = 0$ at the start of our calculation). The top and bottom panels differ in the adopted rate of change of Y_{ν_τ} due to the MSW effect, with $\dot{Y}_{\nu_\tau}^{\text{MSW}}$ [Eq. (17)] and $\dot{Y}_{\nu_\tau}^{\text{MSW}'}$ [Eq. (19)] used for the former and latter, respectively. By the end of our calculation, the Y_{ν_τ} profile is no longer changing significantly. In all cases, the calculation stops at or before $t = 1$ s, when the assumption of static protoneutron star conditions starts to break down. We find that for mixing parameters consistent with current interpretation of and constraints on sterile neutrino dark matter, ν_τ - ν_s and $\bar{\nu}_\tau$ - $\bar{\nu}_s$ mixing can produce Y_{ν_τ} up to ~ 0.1 – 0.2 in protoneutron stars. Our results qualita-

tively resemble those of Refs. [17, 19]. Despite the differences in the adopted protoneutron star conditions and in the approximations used, these results are also similar to each other quantitatively.

In general, each Y_{ν_τ} profile shown in Fig. 3 peaks at a certain radius. This feature occurs because production of Y_{ν_τ} is dominated by escape of $\bar{\nu}_s$ converted from $\bar{\nu}_\tau$ through the MSW effect and this process is the most efficient at the radius where the local $\bar{\nu}_\tau$ energy distribution peaks near the energy for the local MSW resonance. As Y_{ν_τ} increases with time, the potential $V_{\bar{\nu}}$ decreases and for a fixed m_s the local resonance energy $E_R \approx m_s^2/(2V_{\bar{\nu}})$ increases with time. To match a larger E_R with the peak of the local $\bar{\nu}_\tau$ energy distribution, the peak of the Y_{ν_τ} profile shifts to smaller radii where the temperature is higher (T decreases monotonically with radius for $r \gtrsim 8$ km as shown in Fig. 1). Similarly, the resonance energy increases with m_s , and so the peak of the Y_{ν_τ} profile tends to be at smaller radii for larger m_s .

Note that although $\dot{Y}_{\nu_\tau}^{\text{MSW}}$ and $\dot{Y}_{\nu_\tau}^{\text{MSW}'}$ differ by a factor of ~ 4 , the corresponding results on the Y_{ν_τ} profile are rather close, which can be attributed to regulation by the feedback (see Section IV). Note also that the transition between $\bar{\nu}_s$ production through the MSW effect and that through collisions is assumed to occur at $\lambda_R = \delta r$. This abrupt transition leads to the sharp features in some

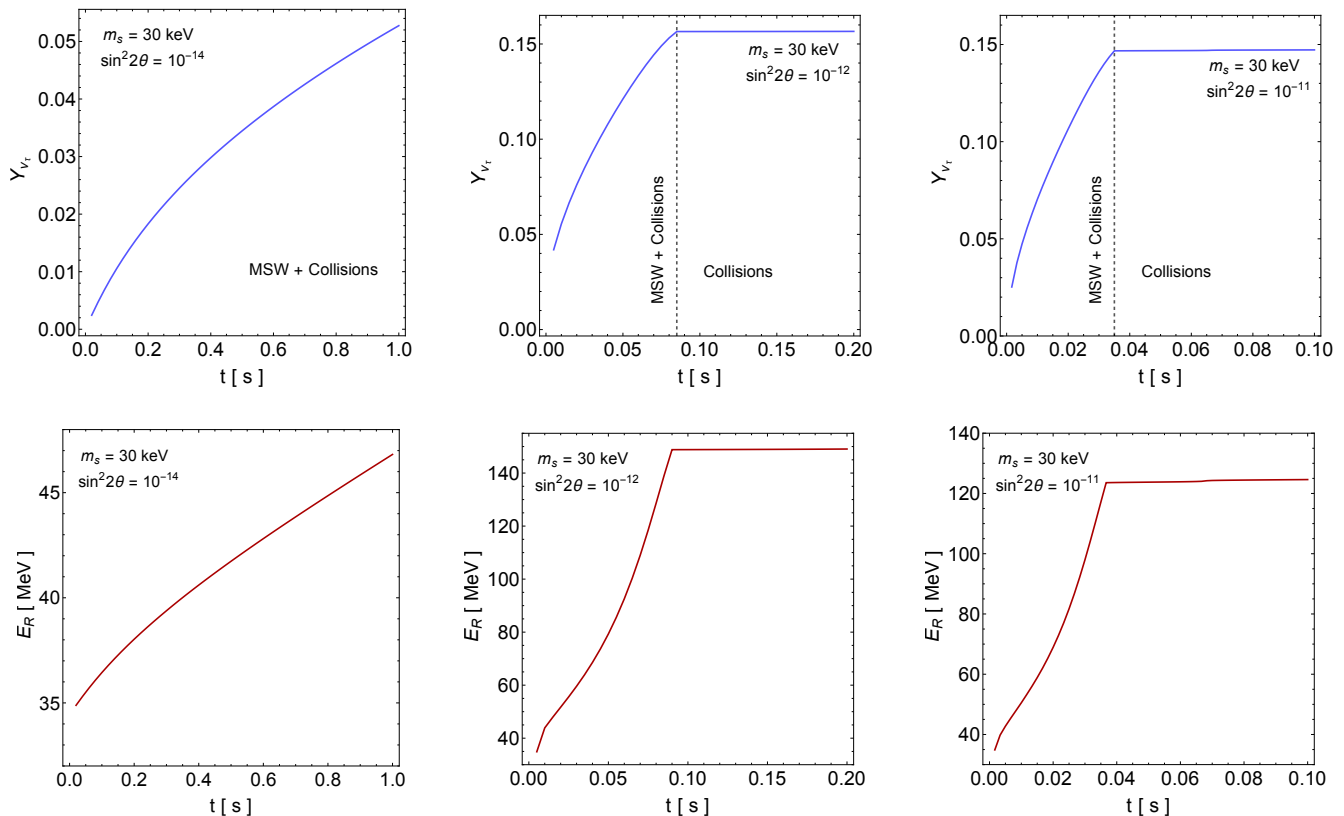


FIG. 4. Time evolution of Y_{ν_τ} (top panels) and the resonance energy E_R (bottom panels) for a zone at $r \approx 8$ km for the indicated mixing parameters ($\dot{Y}_{\nu_\tau}^{\text{MSW}}$ is used).

Y_{ν_τ} profiles shown in Fig. 3.

IV. FEEDBACK AND EVOLUTION OF TAU-NEUTRINO LEPTON NUMBER

To elaborate on the feedback of ν_τ - ν_s and $\bar{\nu}_\tau$ - $\bar{\nu}_s$ mixing in protoneutron stars, we focus on the evolution of Y_{ν_τ} in a specific radial zone. We choose a zone at $r \approx 8$ km with $\rho \approx 4 \times 10^{14}$ g cm $^{-3}$, $T \approx 58$ MeV, $Y_e \approx 0.18$, and $Y_{\nu_e} \approx 0.013$. We take $m_s = 30$ keV along with $\sin^2 2\theta = 10^{-14}$, 10^{-12} , and 10^{-11} , respectively, and show in Fig. 4 the Y_{ν_τ} in this zone as a function of time ($\dot{Y}_{\nu_\tau}^{\text{MSW}}$ is used). In all cases, Y_{ν_τ} initially increases mainly due to escape of $\bar{\nu}_s$ converted from $\bar{\nu}_\tau$ through the MSW effect. This increase of Y_{ν_τ} decreases the potential $V_{\bar{\nu}}$ and hence increases the local resonance energy E_R (see Fig. 4). Consequently, the mean free path λ_R at this energy decreases. Meanwhile, the radial width δr of the resonance region tends to increase due to the flattening of the $V_{\bar{\nu}}$ profile across the zone. When λ_R falls below δr , Y_{ν_τ} production due to the MSW effect turns off and Y_{ν_τ} essentially stops evolving because the rate of production through collisions is small and diffusion is inefficient. This turnoff is clearly seen in Fig. 4 for $\sin^2 2\theta = 10^{-12}$ and 10^{-11} . It occurs earlier for the larger $\sin^2 2\theta$ because δr is proportional to $\sin 2\theta$. For $\sin^2 2\theta = 10^{-14}$, δr is suf-

ficiently small and never exceeds λ_R . Consequently, Y_{ν_τ} production due to the MSW effect persists throughout our calculation in this case. However, this small $\sin^2 2\theta$ also renders the MSW conversion of $\bar{\nu}_\tau$ into $\bar{\nu}_s$ highly inefficient [see Eqs. (6) and (8)]. Consequently, although our calculation is carried out until $t = 1$ s for this case, the final Y_{ν_τ} is still a factor of ≈ 3 smaller than those obtained at $t \approx 0.085$ and 0.035 s for $\sin^2 2\theta = 10^{-12}$ and 10^{-11} , respectively.

In addition to the turnoff for $\lambda_R < \delta r$ discussed above and indicated by the Heaviside step function in Eq. (18), $\dot{Y}_{\nu_\tau}^{\text{MSW}}$ is regulated approximately by the factor $(E_R^3 e^{-E_R/T}) e^{-\eta_{\nu_\tau}}$, which peaks at $E_R = 3T$. For the selected zone with $T \approx 58$ MeV, E_R is always below $3T$ (see Fig. 4) and this factor does not change the above discussion of this zone qualitatively. However, it could effectively turn off the MSW production of Y_{ν_τ} for other zones even when λ_R still exceeds δr . This effective turnoff can occur when E_R increases beyond $3T$ and hence $\dot{Y}_{\nu_\tau}^{\text{MSW}}$ is suppressed exponentially. This suppression is further enhanced by the increase of η_{ν_τ} with Y_{ν_τ} . Therefore, the feedback of ν_τ - ν_s and $\bar{\nu}_\tau$ - $\bar{\nu}_s$ mixing in protoneutron stars always tends to turn off the effects of such mixing.

V. DISCUSSION AND CONCLUSIONS

We have presented a concise and analytical treatment of the processes associated with ν_τ - ν_s and $\bar{\nu}_\tau$ - $\bar{\nu}_s$ mixing in protoneutron stars. These processes include sterile neutrino production through the MSW effect and collisions as well as evolution of the ν_τ -lepton number fraction Y_{ν_τ} through escape of sterile neutrinos and diffusion. We find that for mixing parameters consistent with current interpretation of and constraints on sterile neutrino dark matter of $\mathcal{O}(10)$ keV in mass, ν_τ - ν_s and $\bar{\nu}_\tau$ - $\bar{\nu}_s$ mixing can produce Y_{ν_τ} up to ~ 0.1 – 0.2 in protoneutron stars. This result is consistent with previous studies [17, 19]. In addition, we find that evolution of Y_{ν_τ} is dominated by MSW conversion of $\bar{\nu}_\tau$ into $\bar{\nu}_s$, and that both sterile neutrino production through collisions and Y_{ν_τ} diffusion are inefficient. Mainly through feedback on the potential for $\bar{\nu}_\tau$ - $\bar{\nu}_s$ conversion, the increase of Y_{ν_τ} eventually turns off $\bar{\nu}_s$ production through the MSW effect. Therefore, we confirm conclusions of previous studies [13, 17] that feedback of ν_τ - ν_s and $\bar{\nu}_\tau$ - $\bar{\nu}_s$ mixing tends to turn off the effects of such mixing in protoneutron stars.

In this work, we have made some approximations and assumptions that appear reasonable but are worth discussing. The main approximation is that we have taken radially-propagating neutrinos as representative of flavor evolution governed by the MSW effect in deriving $\dot{Y}_{\nu_\tau}^{\text{MSW}}$. As discussed in Section II A, a full treatment should account for all the directional dependence of $\bar{\nu}_s$ produc-

tion through the MSW effect. Another approximation is the sharp transition between $\bar{\nu}_s$ production through the MSW effect and that through collisions at $\lambda_R = \delta r$. Both the above approximations can be improved by results from future numerical simulations of $\bar{\nu}_\tau$ - $\bar{\nu}_s$ mixing for an isotropic $\bar{\nu}_\tau$ source in a box of linear size comparable to typical $\bar{\nu}_\tau$ mean free path, where collisions occur in a medium of varying density.

The major assumption of this work is that ν_τ - ν_s and $\bar{\nu}_\tau$ - $\bar{\nu}_s$ mixing only affects ν_τ and $\bar{\nu}_\tau$ in protoneutron stars while all the other conditions are unchanged and remain static for ~ 1 s. A self-consistent and full treatment should calculate the dynamical evolution of a protoneutron star by including energy loss through sterile neutrinos and taking into account the modification of ν_τ and $\bar{\nu}_\tau$ distributions by the ν_τ lepton number created through such mixing. Only such a calculation can definitively constrain the mixing parameters associated with sterile neutrino dark matter of $\mathcal{O}(10)$ keV in mass.

ACKNOWLEDGMENTS

We thank George Fuller, Georg Raffelt, Anna Suliga, Irene Tamborra, and Meng-Ru Wu for helpful discussion. We are also indebted to Daniel Kresse and Thomas Janka for providing the supernova model used in this work. This work is supported in part by the National Science Foundation (Grant No. PHY-2020275), the Heising-Simons Foundation (Grant 2017-228), and the U.S. Department of Energy (Grant No. DE-FG02-87ER40328).

-
- [1] A. Kusenko, *Sterile neutrinos: The Dark side of the light fermions*, *Phys. Rept.* **481** (2009) 1 [0906.2968].
 - [2] M. Drewes et al., *A White Paper on keV Sterile Neutrino Dark Matter*, *JCAP* **01** (2017) 025 [1602.04816].
 - [3] K. N. Abazajian, *Sterile neutrinos in cosmology*, *Phys. Rept.* **711-712** (2017) 1 [1705.01837].
 - [4] A. Boyarsky, M. Drewes, T. Lasserre, S. Mertens and O. Ruchayskiy, *Sterile neutrino Dark Matter*, *Prog. Part. Nucl. Phys.* **104** (2019) 1 [1807.07938].
 - [5] B. Dasgupta and J. Kopp, *Sterile Neutrinos*, *Phys. Rept.* **928** (2021) 1 [2106.05913].
 - [6] E. Bulbul, M. Markevitch, A. Foster, R. K. Smith, M. Loewenstein and S. W. Randall, *Detection of An Unidentified Emission Line in the Stacked X-ray spectrum of Galaxy Clusters*, *Astrophys. J.* **789** (2014) 13 [1402.2301].
 - [7] A. Boyarsky, O. Ruchayskiy, D. Iakubovskiy and J. Franse, *Unidentified Line in X-Ray Spectra of the Andromeda Galaxy and Perseus Galaxy Cluster*, *Phys. Rev. Lett.* **113** (2014) 251301 [1402.4119].
 - [8] X. Shi and G. Sigl, *A Type II supernovae constraint on electron-neutrino - sterile-neutrino mixing*, *Phys. Lett. B* **323** (1994) 360 [hep-ph/9312247].
 - [9] H. Nunokawa, J. T. Peltoniemi, A. Rossi and J. W. F. Valle, *Supernova bounds on resonant active sterile neutrino conversions*, *Phys. Rev. D* **56** (1997) 1704 [hep-ph/9702372].
 - [10] J. Hidaka and G. M. Fuller, *Dark matter sterile neutrinos in stellar collapse: Alteration of energy/lepton number transport and a mechanism for supernova explosion enhancement*, *Phys. Rev. D* **74** (2006) 125015 [astro-ph/0609425].
 - [11] J. Hidaka and G. M. Fuller, *Sterile Neutrino-Enhanced Supernova Explosions*, *Phys. Rev. D* **76** (2007) 083516 [0706.3886].
 - [12] G. Raffelt and G. Sigl, *Neutrino flavor conversion in a supernova core*, *Astroparticle Physics* **1** (1993) 165 [astro-ph/9209005].
 - [13] G. G. Raffelt and S. Zhou, *Supernova bound on keV-mass sterile neutrinos reexamined*, *Phys. Rev. D* **83** (2011) 093014 [1102.5124].
 - [14] M. L. Warren, M. Meixner, G. Mathews, J. Hidaka and T. Kajino, *Sterile neutrino oscillations in core-collapse supernovae*, *Phys. Rev. D* **90** (2014) 103007 [1405.6101].
 - [15] M. Warren, G. J. Mathews, M. Meixner, J. Hidaka and T. Kajino, *Impact of sterile neutrino dark matter on core-collapse supernovae*, *Int. J. Mod. Phys. A* **31**

- (2016) 1650137 [1603.05503].
- [16] C. A. Argüelles, V. Brdar and J. Kopp, *Production of keV sterile neutrinos in supernovae: New constraints and gamma-ray observables*, *Phys. Rev. D* **99** (2019) 043012 [1605.00654].
- [17] A. M. Suliga, I. Tamborra and M.-R. Wu, *Tau lepton asymmetry by sterile neutrino emission—moving beyond one-zone supernova models*, *J. Cosmol. Astropart. Phys.* **2019** (2019) 019 [1908.11382].
- [18] A. M. Suliga, I. Tamborra and M.-R. Wu, *Lifting the core-collapse supernova bounds on keV-mass sterile neutrinos*, *JCAP* **08** (2020) 018 [2004.11389].
- [19] V. Syvolap, O. Ruchayskiy and A. Boyarsky, *Resonance production of keV sterile neutrinos in core-collapse supernovae and lepton number diffusion*, *Phys. Rev. D* **106** (2022) 015017.
- [20] S. P. Mikheyev and A. Y. Smirnov, *Resonance enhancement of oscillations in matter and solar neutrino spectroscopy*, *Sov. J. Nucl. Phys.* **42** (1985) 913.
- [21] L. Wolfenstein, *Neutrino oscillations in matter*, *Phys. Rev. D* **17** (1978) 2369.
- [22] W. C. Haxton, *Adiabatic conversion of solar neutrinos*, *Phys. Rev. Lett.* **57** (1986) 1271.
- [23] S. J. Parke, *Nonadiabatic level crossing in resonant neutrino oscillations*, *Phys. Rev. Lett.* **57** (1986) 1275 [2212.06978].
- [24] <https://wwwmpa.mpa-garching.mpg.de/ccsnarchive/>.
- [25] A. Mirizzi, I. Tamborra, H.-T. Janka, N. Saviano, K. Scholberg, R. Bollig et al., *Supernova Neutrinos: Production, Oscillations and Detection*, *Riv. Nuovo Cim.* **39** (2016) 1 [1508.00785].
- [26] R. Bollig, H. T. Janka, A. Lohs, G. Martinez-Pinedo, C. J. Horowitz and T. Melson, *Muon Creation in Supernova Matter Facilitates Neutrino-driven Explosions*, *Phys. Rev. Lett.* **119** (2017) 242702 [1706.04630].
- [27] R. Bollig, W. DeRocco, P. W. Graham and H.-T. Janka, *Muons in Supernovae: Implications for the Axion-Muon Coupling*, *Phys. Rev. Lett.* **125** (2020) 051104 [2005.07141].
- [28] K. C. Y. Ng, B. M. Roach, K. Perez, J. F. Beacom, S. Horiuchi, R. Krivonos et al., *New Constraints on Sterile Neutrino Dark Matter from NuSTAR M31 Observations*, *Phys. Rev. D* **99** (2019) 083005 [1901.01262].
- [29] B. M. Roach, S. Rossland, K. C. Y. Ng, K. Perez, J. F. Beacom, B. W. Grefenstette et al., *Long-exposure NuSTAR constraints on decaying dark matter in the Galactic halo*, *Phys. Rev. D* **107** (2023) 023009 [2207.04572].